Technical Report ICMA-92-175 July, 1992

Multidimensional Computer Simulation of Stirling Cycle Engines

by

C. Hall and T. Porsching

Institute for Computational Mathematics and Applications
Department of Mathematics and Statistics
University of Pittsburgh, Pittsburgh, PA 15260

Final Technical Report
for
NASA-Grant NAG3-1097

MULTIDIMENSIONAL COMPUTER SIMULATION OF STIRLING CYCLE ENGINES

1. Introduction

This report summarizes the activity performed under NASA-Grant NAG3-1097 during 1991. During that period, work centered on the following tasks: (1) To investigate more efficient solvers for ALGAE, (2) To modify the plotting package for ALGAE, and (3) To validate ALGAE by simulating oscillating flow problems similar to those studied by Kurzweg and Ibrahim et. al. [8] - [10].

2. New Solution Methods for ALGAE

This section presents a description of the new direct and iterative solution methods that supplement the original frontal method in the computer program ALGAE. It also discusses a new iterative method for the solution of the discrete energy equations.

2.1. Bordered Banded Solver

The bordered banded solver implemented in ALGAE makes use of customized CRAY Y/MP routines. A general reference for direct solver strategies may be found in, for example, [1]. The ALGAE algorithm is basically a block Gaussian elimination strategy which exploits the structure of the dual variable system and the Cray library routines in LAPACK, [2]. Also, unlike the frontal solver in ALGAE, the bordered banded solver makes no use of disk storage for problems as large as 10,000 flow cells. Timing comparisons are included which indicate a speedup factor of 5 to 6 for moderate size problems and a factor of 4 to 5 for larger problems when compared with an *optimized* frontal solver. These factors are considerably larger (50 to 200) when the bordered banded solver times are compared to those of the *original* (single precision) ALGAE frontal solver.

2.1.1. Reordering of the equations and dual variables

The system that is solved at each time step in ALGAE is composed of equations having two separate nonzero structures. Normally an equation in the dual variable system has a zero-nonzero structure which is similar to that resulting from the 13 point finite difference stencil approximating the biharmonic operator. That is, there are at most 13 nonzero entries in the equation, and the semi-bandwidth is generally 2N for an N by N flow cell problem. The second type of equation arises when there are obstructions in the flow region or if the flow is pressure driven. In such cases there are equations in which there are generally many more nonzero entries and these may occur outside the band of width 4N. In terms of network terminology, cycles or countries that are composed of 4 or less links give rise to equations that are of the first type, while cycles that circumscribe obstacles or connect pressure specified boundary segments may give rise to equations of the second type.

The first modification to the solution strategy in ALGAE is a reordering of the unknown dual variables and equations so that the more complex type 2 equations occur last in the system. The resulting system is then bordered banded and can be written as

$$B\ X = K\,,$$

where B is a block matrix of the form

$$B = \begin{bmatrix} B_{11} & B_{12} \\ B_{21} & B_{22} \end{bmatrix}.$$

The matrix B_{11} is banded and very sparse, the dimension of B_{22} is usually quite small, and the matrices in the border (B_{12}, B_{21}, and B_{22}) are generally dense. Note that B_{22} may be void, i.e., the matrix B on occasion may be banded. It is assumed that $X = (X_1, X_2)$ and $K = (K_1, K_2)$ are partitioned consistently with the partitioning of B.

2.1.2. Storing nonzero entries

To eliminate the use of disk I/O during the solution of the dual variable system, the positions (I, J) of possible nonzero entries in the dual variable system are calculated once and for all. These positions are the same for each time step of the transient. Given these positions, only the nonzero entries of the system are calculated.

2.1.3. Bordered banded solution algorithm

The bordered banded algorithm used is contained in the software package BORMAT available from the Pittsburgh Supercomputer Center [3]. Note that the BLAS, LAPACK and LINPACK routines used in BORMAT are available on the CRAY in SCILIB. (The LAPACK option is used in BORMAT).

The bordered banded system is factored and the resulting factored system is then solved. The process is as follows:

(1) B_{11} is factored and the L-U factors $L_{11}U_{11}$ are stored.

(2) The system

$$L_{11}U_{11}\ Z = -B_{12},$$

is solved and B_{12} is overwritten with the result.

(3) Gaussian elimination of the two block rowed system requires the calculation of

$$B'_{22} = B_{22} - B_{21}(L_{11}U_{11})^{-1}\ B_{12} = B_{22} + B_{21}Z$$

using the Z in step (2). The result is stored in B_{22}.

(4) The new (2,2) block determined in step (3)

$$B'_{22} = L_{22}U_{22},$$

is factored and the result stored in the same space.

(5) The subsystem

$$L_{11}U_{11}\ Y_1 = K_1.$$

is solved.

(6) K_2 is replaced by $K_2 - B_{21}\ Y_1$.

(7) The subsystem

$$(L_{22}U_{22})\ X_2 = K_2.$$

is solved.

(8) The solution X_1 is calculated as

$$X_1 = Y_1 + B_{21}X_2 .$$

2.1.4. Performance Data

Four data files were used to initially test the modified ALGAE solution options. The first problem involved a preheater section geometry, the second dealt with flow through an aircraft compartment containing obstacles, and the third and fourth were driven cavity geometries. The following are the statistics for these problems. NOB denotes the dimension of B_{22}.

Problem	Flow cells	Dual variables	NOB	Semi-bandwidth
Preheater	758	700	1	45
Aircraft compartment	1174	1065	3	60
Small cavity	2500	2401	0	98
Large cavity	10000	9801	0	198

Three solvers were tested; the original frontal solver, an optimized version of the frontal solver, and finally the bordered banded solver described above. The following are timings for a CRAY Y/MP using one processor. (This enhances the performance of the bordered banded solver and has very little effect on that of the frontal solver.)

Each problem was run for ten steps. The following table lists the average time in seconds to solve the dual variable system for each of the four problems. Due to the excessive cost, the large cavity problem timings for the original frontal scheme (designated *) are for a single step. Also included are the ratios of the solve times for the optimized frontal solver to those of the bordered banded solver.

Average Time to Solve One System				
Problem	Original frontal	Optimized frontal	Bordered banded	Ratio
Preheater	10.52	0.51	0.05	9.3
Aircraft compartment	16.94	0.82	0.09	8.3
Small cavity	38.46	2.04	0.32	6.4
Large cavity	191.08*	14.22	3.52	4.0

The next table contains the CPU charges on the Y/MP for the ten steps of each of the runs. This includes setup, solution times and I/O for the entire run. The CPU time (designated **) for the original frontal solver was determined by multiplying that for a single step by ten. As above, the ratios of these

times for the optimized frontal and bordered banded solvers are also given. Note that there is a one time additional cost for the setup of the bordered-banded solver. These ratios would increase if this cost was amortized over more steps.

Total CPU Time Charged				
Problem	Original frontal	Optimized frontal	Bordered banded	Ratio
Preheater	108.29	7.49	2.99	2.5
Aircraft compartment	171.68	10.52	3.45	3.0
Small cavity	388.26	24.09	7.38	3.3
Large cavity	1969.5**	154.45	53.13	2.9

In addition to the above data, note that the wall clock times for the optimized frontal method were consistently 2 to 3 times greater than those for the bordered banded solver. Presumably this is a reflection of the need for disk I/O in the former. Of course, the wall clock time depends on the computing environment and the level of usage of the machine at any given time.

2.2. Iterative Solvers

The iterative solvers that have been incorporated into the ALGAE program are based on a package of preconditioned conjugate gradient methods developed by the Mathematical Software Research Group at Cray Research, Inc.. A discussion of the package and details of its usage are given in [4] and [5].

The NAMELIST/START/ variable ISOLV selects the type of solver to be used in ALGAE as follows:

$$\text{ISOLV} = \begin{cases} 0 & \text{optimized frontal method (default)} \\ 1 & \text{bordered–banded direct method} \\ 2 & \text{pure iterative method} \\ 3 & \text{hybrid method} \end{cases}$$

Note that in addition to the pure iterative solver, a hybrid solver is included that incorporates selected calls to the bordered-banded direct solver. The intention is to combine the computational efficiency of an iterative solver with the robustness of a direct solver. The strategy controlling the use of these solvers is discussed in section 1.2.3.

2.2.1. Data Structure

Let $A\mathbf{x} = \mathbf{b}$ denote the dual variable system. The *sparse column format* is used to represent the coefficient matrix A. In this format the row indices of the (potentially) nonzero entries of the j-th column are stored in ascending order. The corresponding values are also stored. There is also a pointer array containing pointers to the locations of the row index and value of the first nonzero entry in each of the columns.

2.2.2. Dual Variable System Generation

The dual variable coefficient matrix A is a product $A = C^T Q C$, where C is a fundamental matrix for the network defined by the finite difference mesh, and Q is the coefficient matrix of the discrete momentum equations. Thus, if $A = [a_{ij}]$, $C = [c_{km}]$ and $Q = [q_{\mu\nu}]$, then

$$a_{ij} = \sum_{\mu,\nu} c_{\mu i} q_{\mu\nu} c_{\nu j} .$$

Now the data structures of ALGAE are such that the matrix C is defined by the link numbers. Therefore, A is generated by determining for each μ, ν pair the i, j pairs for which a_{ij} receives a contribution of the form $c_{\mu i} q_{\mu\nu} c_{\nu j}$, and then accumulating the sums.

The driver for the iterative solver uses an array to map the contributions to the a_{ij} onto their proper locations in the array containing the matrix values. This avoids conditional testing and enhances the vectorization process.

2.2.3. Program Control

For the pure iterative solver, the designated method is used with (or without) user selected preconditioning at each time step. If a fatal error is detected during the course of an iteration, or if the solution has not satisfied the convergence criterion in the user designated maximum number of iterations, a message is written and the computations are terminated.

For the hybrid solver, the solution is computed using the bordered-banded direct solver at the first time step and the preconditioning toggle is turned on. For each subsequent time step, an iterative solution is attempted. An incomplete LU factorization is computed to precondition the system if the

toggle is on, and the toggle is then turned off. Otherwise, the iterative method uses the most recently computed incomplete LU factors as the preconditioner. The iterative solution is accepted provided that an internal convergence criterion is satisfied *and provided that* $\|A\,x^* - b\|_\infty \le 10^{-4} / \|x^*\|_\infty$, where x^* is the iterative solution. Otherwise, the system is resolved using the bordered-banded direct solver and the preconditioning toggle is turned on.

2.2.4. Performance Data

The first problem considered is the preheater problem. This is a modified version of the sample problem given in Section 6, Volume 2 of [6]. There are 750 flow cells and 700 dual variables. The timings in the following table are based on the average solution time over thirty consecutive time steps using a step size of .5 seconds. The original frontal method required 10.52 sec/solve, while the optimized frontal method took .51 sec/solve. The column headed RATIO gives the ratio of the optimal frontal solve time to that of the iterative solve time, and the last column gives the maximum pressure drop (psi) around the cycles after the final time step. This quantity would be zero for an exact solution, and so it may be used as a measure of the accuracy of the iterative solution.

Method	ISOLV	Sec/Solve	RATIO	Max. Loop Δp
CGS	2	.15	3.4	$.24\times10^{-4}$
	3	.17	3.0	$.82\times10^{-9}$
GMR	2	.14	3.6	$.37\times10^{-3}$
	3	.19	2.7	$.92\times10^{-9}$

The second set of sample timings corresponds to a large Poiseuille-type problem with heat added to the central portion of the channel. There are 10000 flow cells and 9900 dual variables. The sample times of the following table are based on the average solution time over 10 consecutive time steps using a step size of 1.0. The original and optimized frontal methods required 193.5 and 15.3 sec/solve. The conventions used in describing the previous table again apply.

Method	ISOLV	Sec/Solve	RATIO	Max. Loop Δp
CGS	2	3.42	4.5	$.12\times10^{-5}$
	3	4.34	3.5	$.14\times10^{-9}$
GMR	2	3.04	5.0	$.48\times10^{-6}$
	3	4.83	3.2	$.14\times10^{-9}$

2.3. Energy Equation

The original point Gauss-Seidel method used in ALGAE to solve the discrete energy equations has been replaced by the point Jacobi method. For model problems the asymptotic rate of convergence of the Jacobi method is not as large as that of the Gauss-Seidel method. (See, for example, [7].) However, it is amenable to vectorization, whereas the Gauss-Seidel method is not.

Sample timings were made on the two problems used to test the iterative solvers. The following table shows that for these problems the new method resulted in an average speed-up factor (RATIO) that is slightly greater than three.

Problem	No. Time Steps	Avg. Solve Times (Sec.)		RATIO
		Gauss-Seidel	Jacobi	
Preheater	30	.044	.013	3.4
Heated Channel	10	.328	.108	3.04

3. Modification of Plotting Package for ALGAE

The original plotting package for ALGAE assumed that all walls were adiabatic. This was also the assumption made in the fluid modeling by ALGAE, and was reasonable for thermal transfer in reactor components. The ability to allow for conduction from solid walls was added to the code ALGAE some years ago, but the plotting package was not changed to adequately display temperature distributions near solid walls. As such, some thermal contours, while completely accurate one flow cell from the wall, would terminate orthogonal to the wall. The plotting package has been updated this year and now displays the correct contour levels up to and including the walls.

4. Oscillating Flow in a Regenerator Component

As part of the validation of ALGAE for Stirling Engine simulations, we consider a model of a parallel plate regenerator similar to that studied by Ibrahim et. al. [8], [9]. Figure 1 shows a schematic of the geometry and lists the assumed physical properties of the working gas (Helium) and wire[1]. Also shown are the boundary conditions and mesh spacings used by ALGAE. Note that the angular frequency and amplitude of the oscillating pressure drop forcing function are 412.5 sec^{-1} and .0349 psi

[1] These were suggested by M. Ibrahim in a private communication, dated Dec. 11, 1991.

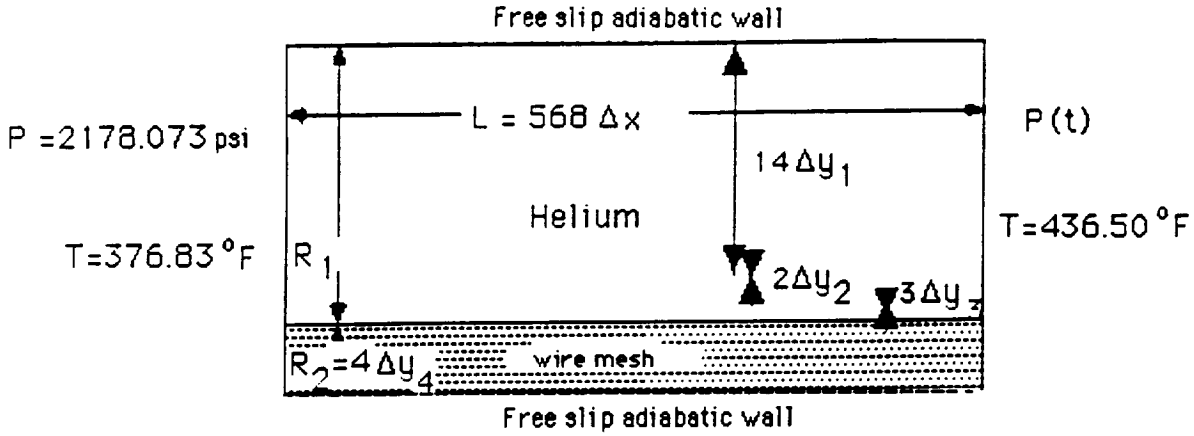

R_1 = radius of channel = .218667 E-03 ft

R_2 = radius of wire = .41666 E-04 ft

L = length of channel = .3 E-02 ft

Δy_1 = .13975 E-04, Δy_2 = .57545 E-05, Δy_3 = .38363 E-05, Δy_4 = .10417 E-04

Δx = .17328 E-04 ft

Helium Properties:

Molecular weight : 4.002
Specific Heat: 1.24 BTU/lbm °F
Thermal conductivity: 3.53 E-05 BTU/sec ft °F
Viscosity: 0.185 E-04 lbm/ft sec
Density: 0.93767 lbm/ft^3

Steel Properties:

Specific Heat: 0.1117 BTU/lbm °F
Thermal conductivity: 0.215 E-02 BTU/sec ft °F
Density: 514.28 lbm/ft^3

$$P(t) = 2178.073 + 0.0349 \cos (\pi / 2 + 412.5\, t)$$

Figure 1. Parallel plate regenerator.

respectively. This corresponds to a Valensi number, *Va*, of 1 and maximum Reynolds number, Re_{max}, of 262, and facilitates comparison of the present results with those of [9], Figures 1 and 2, where these quantities were 1 and 200. Recall that *Va* and Re_{max} are defined as follows:

$$Va = \frac{\omega D_h^2}{4\nu}, \quad Re_{max} = \frac{\bar{u}_{max} D_h}{\nu},$$

where ω is the frequency, D_h the hydraulic diameter, ν the kinematic viscosity, and $\bar{u}_{max}$ the maximum over one half cycle of the average axial velocity.

Unlike the one dimensional numerical methods reported in [8] and [9], ALGAE solves the full (unsteady) two dimensional Navier-Stokes and heat convection-conduction equations. Thus, radial convection, conduction, and momentum effects are directly accounted for.

Figures 2 and 3 show axial Velocity and Temperature profiles as a function of the radial distance measured from the centerline of the channel. The 12 curves shown on each figure correspond to increments of 30° in the crank angle as indicated by the accompanying key. These plots were made after a start up transient of about 1.25 sec. They should be compared with Figures 1 and 2 of [9] which give analogous plots of these quantities for the numerical model used in that work.

As shown in Figure 2, the time dependent behavior of the channel centerline axial velocity is cyclic with an amplitude of about 18 ft/sec. This should be compared with the analogous result of [9], Figure 1, where the amplitude is ≈13 ft/sec. The temperature variation of the Helium given by Figure 3 is approximately 49°F about a temperature of 406 °F, whereas that of Figure 2 in [9] is ≈31°F about 408 °F. On the other hand the temperature variation in the wire shown in Figure 3 is about 2 °F, while that of Figure 2 in [9] is ≈14°F. Since the main mechanism for heat transfer in the Helium is convection, the 49°F variation in the gas would presumably be reduced if Re_{max} were reduced from 262 to 200. This will probably also reduce the variation in the wire. The two dimensional calculations do not yield as rapid a response of the temperature at the gas-wire interface as those of [9]. This may be due to a poor resolution of the boundary layer because of the coarseness of the spatial mesh near the interface.

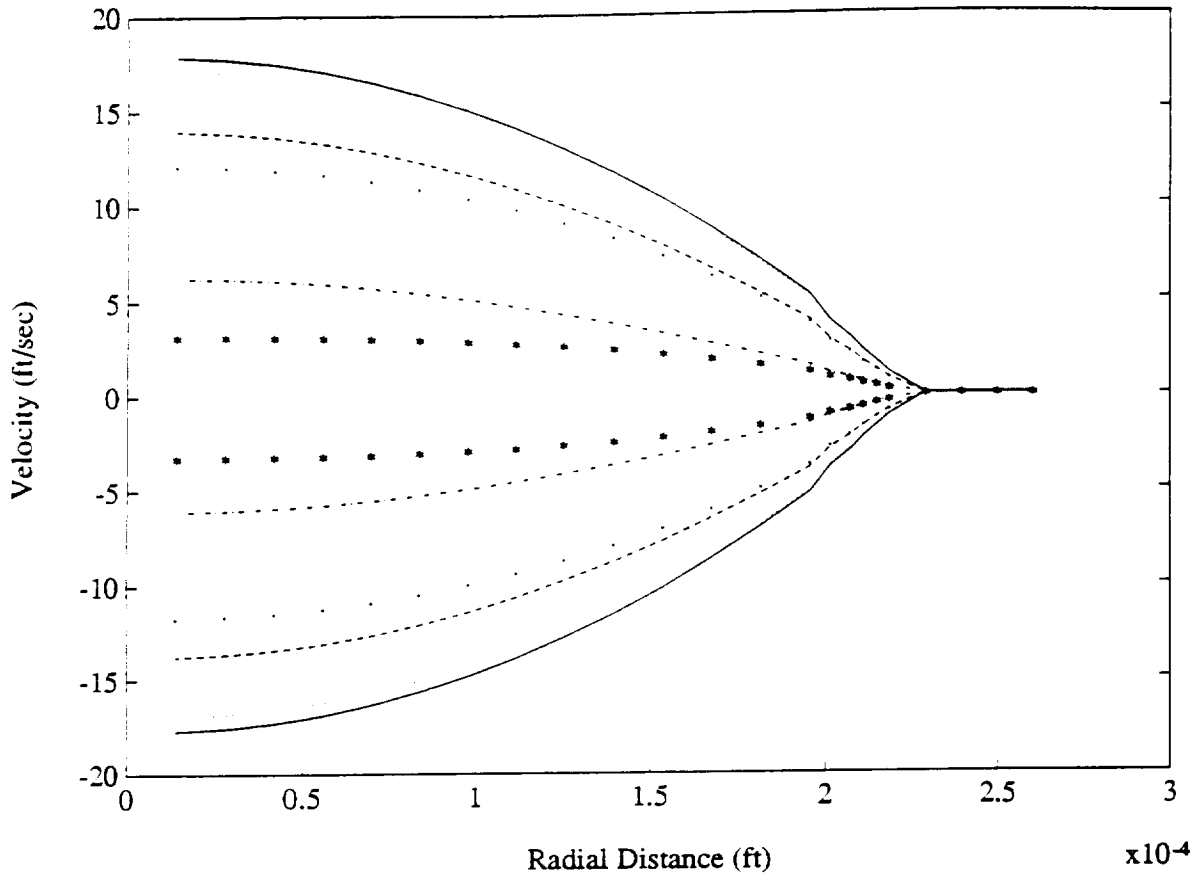

KEY

Symbol	Crank Angle (deg)	℄ Value (ft/sec)
———	210, 30	17.9, -17.7
.....	180, 0	17.21, -16.94
– – –	240, 60	13.9, -13.74
. . .	150, 330	12.13, -11.69
— - —	270, 90	6.25, -6.09
*****	120, 300	3.18, -3.21

Figure 2. Axial velocity profiles

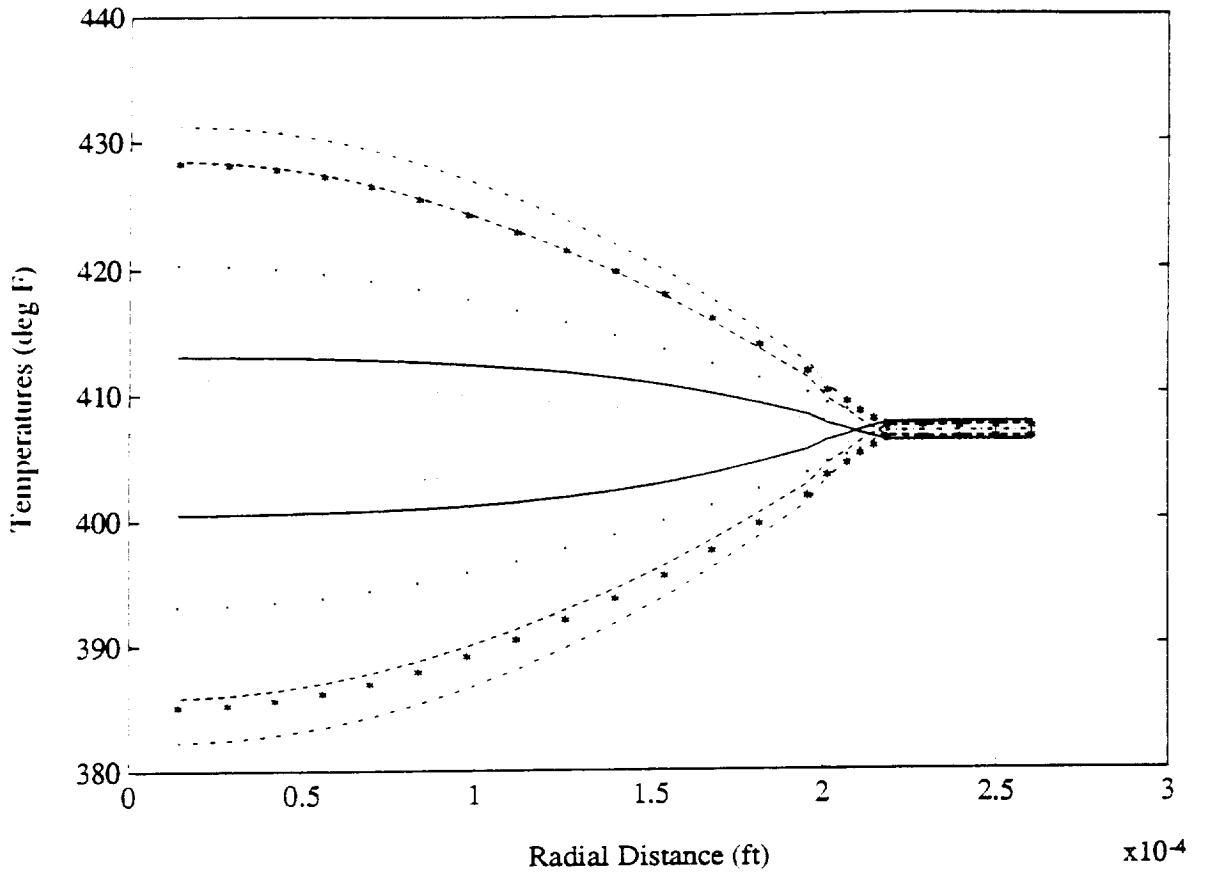

KEY

Symbol	Crank Angle (deg)	℄ Value (deg F)
———	210, 30	400.51, 413.09
.....	180, 0	411.31, 402.33
- - - -	240, 60	385.83, 428.5
. . . .	150, 330	420.40, 393.16
— - —	270, 90	382.28, 431.29
* * * * *	120, 300	428.34, 385.12

Figure 3. Temperature profiles

References

1. I. S. Duff, A. M. Erisman, and J. K. Reid, *Direct Methods for Sparse Matrices*, Clarendon Press, Oxford University Press, 1986.

2. *UNICOS Math and Scientific Library Reference Manual* SR-2081 6.0, Cray Research, 1991.

3. *PSCDOC:BORMAT.DOC*, Pittsburgh Supercomputing Center, May, 1991.

4. M. Heroux, P. Vu and C. Yang, "A Parallel Preconditioned Conjugate Gradient Package for Solving Sparse Linear Systems on a Cray Y-MP," Cray Research, Inc., preprint.

5. UNICOS Math and Scientific Library Reference Manual SR-2081 6.0, Vol 3, Cray Research, Inc., Mendota Heights, MN, 1991, pp 227-243.

6. R. S. Dougall, C. A. Hall and T. A. Porsching, "DUVAL: A Computer Program for the Numerical Solution of Two-Dimensional, Two-Phase Flow Problems, Vols. 1-3,", Report NP-2099, Electric Power Research Institute, Palo Alto, CA, 1982.

7. L. A. Hageman and D. M. Young, *Applied Iterative Methods*, Academic Press, New York, 1981.

8. M. B. Ibrahim, R. C. Tew and J. E. Dudenhoefer, "Two-dimensional Numerical Simulation of a Stirling Engine Heat Exchanger", Proc. 24th IECEC, Paper 899536, Washington DC, 1989.

9. M. B. Ibrahim, R. C. Tew and J. E. Dudenhoefer, "Further Two-dimensional Code Development for Stirling Space Engine Heat Components", Proc. 25th IECEC, Reno, NV, 1990, Vol. 6, pp 329-335.

10. U. H. Kurzweg, "Enhanced Heat Conduction in Oscillating Viscous Flows Within Parallel-Plate Channels", *J. Fluid Mech.*, 156,291-300, 1985.